ACS NANO

Cite This: ACS Nano 2019, 13, 2262–2273

www.acsnano.org

ARTICLE

Engineering Nanowire-Mediated Cell Lysis for Microbial Cell Identification

Takao Yasui,[*,†,‡,§] Takeshi Yanagida,[*,⊥,∥] Taisuke Shimada,[†] Kohei Otsuka,[†] Masaki Takeuchi,[†] Kazuki Nagashima,[⊥] Sakon Rahong,[‡,#] Toyohiro Naito,[¶] Daiki Takeshita,[†] Akihiro Yonese,[†] Ryo Magofuku,[†] Zetao Zhu,[⊥] Noritada Kaji,[‡,§,▽] Masaki Kanai,[⊥] Tomoji Kawai,[*,∥] and Yoshinobu Baba[*,†,‡,○,◆]

[†]Department of Biomolecular Engineering, Graduate School of Engineering and [‡]ImPACT Research Center for Advanced Nanobiodevices, Nagoya University, Furo-cho, Chikusa-ku, Nagoya 464-8603, Japan

[§]Japan Science and Technology Agency (JST), Precursory Research for Embryonic Science and Technology (PRESTO), 4-1-8 Honcho, Kawaguchi, Saitama 332-0012, Japan

[⊥]Institute of Materials Chemistry and Engineering, Kyushu University, 6-1 Kasuga-Koen, Kasuga, Fukuoka 816-8580, Japan

[∥]Institute of Scientific and Industrial Research, Osaka University, 8-1 Mihogaoka-cho, Ibaraki, Osaka 567-0047, Japan

[#]College of Nanotechnology, King Mongkut's Institute of Technology Ladkrabang, Chalongkrung Rd., Ladkrabang, Bangkok 10520, Thailand

[¶]Department of Material Chemistry, Graduate School of Engineering, Kyoto University, Katsura, Nishikyo-ku, Kyoto 615-8510, Japan

[▽]Department of Chemistry and Biochemistry, Graduate School of Engineering, Kyushu University, Moto-oka 744, Nishi-ku, Fukuoka 819-0395, Japan

[○]Health Research Institute, National Institute of Advanced Industrial Science and Technology (AIST), Takamatsu 761-0395, Japan

[◆]College of Pharmacy, Kaohsiung Medical University, Kaohsiung 807, 80708 Kaohsiung City, Taiwan, R.O.C.

Supporting Information

ABSTRACT: **Researchers have demonstrated great promise for inorganic nanowire use in analyzing cells or intracellular components. Although a stealth effect of nanowires toward cell surfaces allows preservation of the living intact cells when analyzing cells, as a completely opposite approach, the applicability to analyze intracellular components through disrupting cells is also central to understanding cellular information. However, the reported lysis strategy is insufficient for microbial cell lysis due to the cell robustness and wrong approach taken so far (*i.e.*, nanowire penetration into a cell membrane). Here we propose a nanowire-mediated lysis method for microbial cells by introducing the rupture approach initiated by cell membrane stretching; in other words, the nanowires do not penetrate the membrane, but rather they break the membrane between the nanowires. Entangling cells with the bacteria-compatible and flexible nanowires and membrane stretching of the entangled cells, induced by the shear force, play important roles for the nanowire-mediated lysis to Gram-positive and Gram-negative bacteria and yeast cells. Additionally, the nanowire-mediated lysis is readily compatible with the loop-mediated isothermal amplification (LAMP) method because the lysis is triggered by simply introducing the microbial cells. We show that an integration of the nanowire-mediated lysis with LAMP provides a means for a simple, rapid, one-step identification assay (just introducing a premixed solution into a device), resulting in visual chromatic identification of microbial cells. This approach allows researchers to develop a microfluidic analytical platform not only for microbial cell identification including drug- and heat-resistance cells but also for on-site detection without any contamination.**

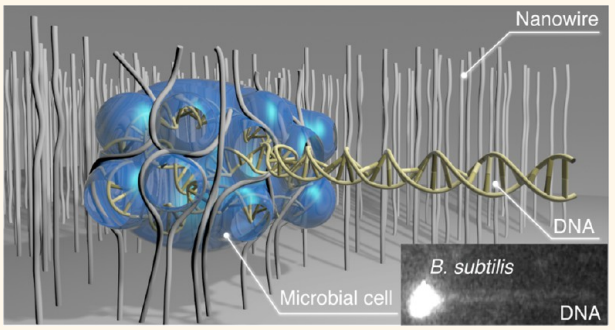

KEYWORDS: *nanowires, microfluidics, nanowire-mediated lysis, microbial cell, intracellular analysis, loop-mediated isothermal amplification*

Inorganic nanowires have been found to hold great promise for analyzing cells or intracellular components,[1] by such techniques such as three-dimensional intracellular record-

Received: November 25, 2018
Accepted: January 25, 2019
Published: February 13, 2019

DOI: 10.1021/acsnano.8b08959
ACS Nano 2019, 13, 2262–2273

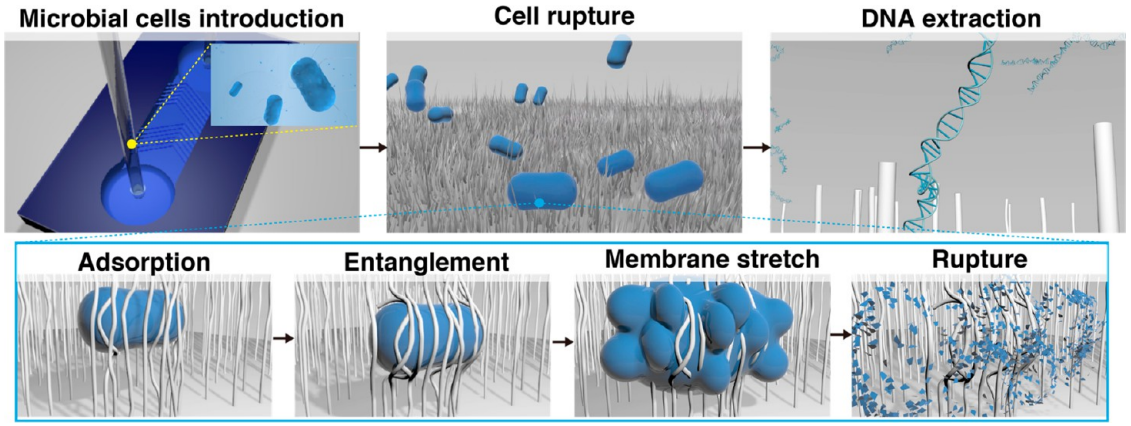

Figure 1. Schematic illustrations for nanowire-mediated lysis of microbial cells. There is a nanowire-mediated membrane rupture of microbial cells, followed by DNA extraction from the microbial cells.

ing,[2] syringe-injectable electronics,[3] intracellular component isolation[4] and separation,[5] and intracellular reagent delivery.[6] These studies have utilized features of the nanowires, including their nanometer-scale diameter size, rigidity, high aspect ratio, and capability to function as electrophysiological probes.[2−10] These studies were aimed at preserving the intact living cells and intracellular components *via* a stealth effect of nanowires toward cell surfaces and components, for example, nanowire penetration into cells without compromising cell viability. As a completely opposite approach, an analysis of intracellular components through lysing cells is an important way to obtain cellular information in molecular biology, especially for microbial cells. However, the applicability of penetration of nanowire tips into microbial cells has been thought to be doubtful due to their toughness to external forces (Young's modulus, ∼100 MPa),[11,12] and therefore, this limitation has hindered the versatility of the inorganic nanowires for analyzing cells or intracellular components.

Microbial cell lysis is an essential analytical methodology for microbial genome sequencing from single cells,[13,14] since genomic DNA analysis from single microbial cells is expected to uncover and broaden uncharted branches of the tree of life, that is, microbial dark matter. Among the existing lysis methods for microbial cells,[15,16] thermal, chemical, optical, electrical, and mechanical lysis in a microfluidic platform are candidates for the lysis applicability to all types of microbial cells. However, these lysis methods have suffered from various issues, including: insufficient thermal diffusion;[17] difficult regent delivery and difficult reagent separation;[18,19] expensive and complex setups;[20,21] bubble formation;[22,23] and complex nanofabrication processes.[24−27] A concept for nanowire-mediated microbial cell lysis is expected to provide a good way to address the inherent difficulties in these lysis methods. Use of nanowires adds an additional feature to conventional cell lysis, leading to significantly enhanced lysis performance and overcoming the above issues.

A nanowire-assisted cancer cell lysis by utilizing ZnO nanowires (*ca.* 100 nm in diameter) has been reported by Kim *et al.*[28] and So *et al.*,[29] in which they used nanowires to anchor cells and ruptured the cells anchored in the nanowires by the shear force. Their studies and that of Ning *et al.*[30] were intended to rupture the cells *via* a cytotoxic effect of nanowires toward the cell surfaces, that is, by nanowire penetration into cells with tearing of the cell membrane[28,29] or inducing apoptosis,[30] or both of them. Since cancer cells are soft (Young's modulus, ∼1 kPa),[31] it is considered that the cell rupture has been initiated by penetration of nanowire tips into the cellular membrane. The reported lysis strategy has had the intention of fabricating more rigid nanowires for nanowire penetration into a cell membrane. However, this strategy is insufficient for microbial cell lysis due to the cell robustness. The rigidity of microbial cells does not allow nanowires to penetrate into the cell membrane, and therefore, from the perspective of the lysis applicability to all types of microbial cells, our strategy to accomplish nanowire-mediated cell lysis should be based on a different rupture mechanism rather than the conventional mechanism (a penetration of nanowire tips into cells).

Here we propose a nanowire-mediated lysis method for microbial cells by introducing the rupture approach initiated by the cell membrane stretching; in other words, the nanowires do not penetrate the membrane, but rather they break the membrane between the nanowires. Figure 1 shows a schematic of our proposed concept to rupture microbial cells by stretching the cell membrane *via* the thin and bacteria-compatible nanowires, that is, nanowire-mediated mechanical lysis. This rupture mechanism is initiated by cell adsorption onto the nanowires, it proceeds by cell entanglement with the nanowires, and it is completed by non-uniform stretching of the cell membrane in the spaces between the nanowires while applying external driving forces (an electric field and fluid flow), leading to irreversible membrane rupture. The role of the external driving forces is to provide an external force to press the cells into the spacing between nanowires, thus enhancing the shear force applied to the cell membrane. A key factor for membrane rupture is the degree of stretching that is determined by a combination of cell rigidity,[32−34] material compatibility with bacteria for their adsorption, nanowire flexibility for bacteria entanglement, and the shear force for membrane stretching; the mechanism is inherently different from the nanowire tip penetration mechanism. The rupture mechanism evokes an image that the more bacteria-compatible materials and flexible nanowires would have a stronger ability to rupture microbial cells. Since it is well-known that SiO_2 has more biocompatibility[35] and thinner nanowires have higher flexibility,[36,37] we anticipated that the thinner nanowires with an SiO_2 surface coating would significantly enhance bacteria adsorption and entanglement. In this paper, first, we fabricated 30 nm diameter and 2 μm length nanowires (∼60 wires/μm^2) with the SiO_2 surface coating (10 nm diameter SnO_2 nanowires with a 10 nm-

DOI: 10.1021/acsnano.8b08959
ACS Nano 2019, 13, 2262−2273

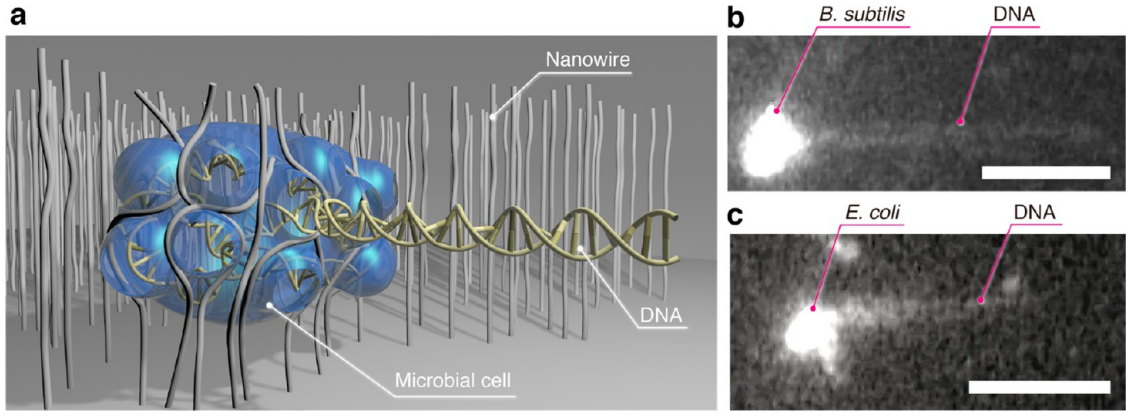

Figure 2. DNA extraction of microbial cells using nanowires in a microchannel. (a) A schematic illustration showing nanowire-mediated lysis. (b) A fluorescence image showing DNA extraction from a single cell of *B. subtilis*; scale bar, 10 μm. (c) A fluorescence image showing DNA extraction from a single cell of *E. coli*; scale bar, 10 μm.

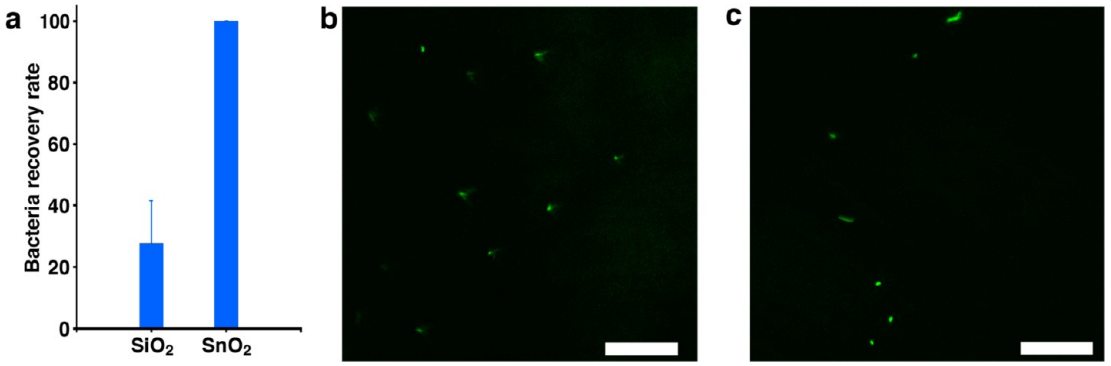

Figure 3. Antibacterial test for SiO_2 and SnO_2 substrates. (a) Bacteria recovery rate for SiO_2 and SnO_2 substrates. Error bars show the standard deviation for a series of measurements ($N = 3$). (b, c) Confocal microscope images that show *E. coli* on SiO_2 substrates, respectively, without and with 10 mL PBS washing process; scale bars, 30 μm. Some bacteria were observed on SiO_2 substrates even though they underwent the washing processes. The washing processes could not remove all bacteria from the SiO_2 substrates.

thick SiO_2 shell) (Figure S1) to facilitate membrane stretching, and we followed that stretching by rupture of microbial cells.

RESULTS AND DISCUSSION

DNA Extraction *via* Nanowire-Mediated Lysis. To demonstrate that the DNA extraction *via* nanowire-mediated rupture is applicable to microbial cells (Figure 2a), we used *Bacillus subtilis* and *Escherichia coli* as a typical example of Gram-positive and Gram-negative bacteria, respectively (Supporting Information). The Gram-positive bacteria have strong resistivity to physical damage due to their thick (20−80 nm) peptidoglycan layer,[38] and the Gram-negative bacteria have strong resistivity to chemical damage due to their outer membrane.[39] The cells were introduced by capillary force onto the nanowires in a microchannel, and the cells contacted with the oxide nanowire surface (Figure S2). Various imaging results showed that the cells were not ruptured by the capillary force (Figure S3). After applying an electric field of 500 V/cm, the nanowires exhibited DNA extraction from *B. subtilis* and *E. coli* (Figure 2b,c). We determined the molecules extracted by the observed cell lysis were DNA molecules *via* monitoring the time series data of fluorescence intensity of the extracted molecules with fluorescence labeling (Figure S4 and Supplementary Movie 1). These results highlight our demonstration of a methodology for nanowire-mediated lysis to extract microbial DNA molecules by 30 nm diameter nanowires while applying an electric field.

Nanowire-Mediated Lysis Mechanism (Bacteria-Compatibility, Flexibility, and External Driving Forces). Based on our proposed concept (Figure 1), the present nanowire-mediated lysis has three steps: adsorbing cells onto the nanowires, entangling cells with the nanowires, and stretching the cell membrane in the spaces between the nanowires while applying external driving forces. We carried out a Japanese Industrial Standards (JIS)-based antibacterial test (JIS Z2801:2010, which is based on ISO 22196, Supporting Information) for bacteria compatibility of nanowire materials. Then, we examined the effect of nanowire flexibility (specifically, the wire diameter) on bacteria entanglement by SEM observations of microbial cells on the nanowires with different diameters, and we investigated the effect of the external driving forces (applied electric fields) on membrane rupture by fluorescently observing the rupture event. Considering the features of the present nanowires and the effect of the external driving forces, we concluded that the present nanowire-mediated lysis could extract microbial DNA molecules *via* the three steps.

The first step for adsorbing cells onto the nanowires was evaluated by the antibacterial test showing that SiO_2 and SnO_2 materials (the nanowire shell and core materials) had good bacteria compatibility, and SiO_2 enhanced bacteria adsorption (Figure 3). For fabrication of SnO_2 substrates, a 100 nm-thick SnO_2 layer was deposited on a SiO_2 substrate (50×50 mm^2) by atomic layer deposition (Figure S5). The antibacterial test

DOI: 10.1021/acsnano.8b08959
ACS Nano 2019, 13, 2262−2273

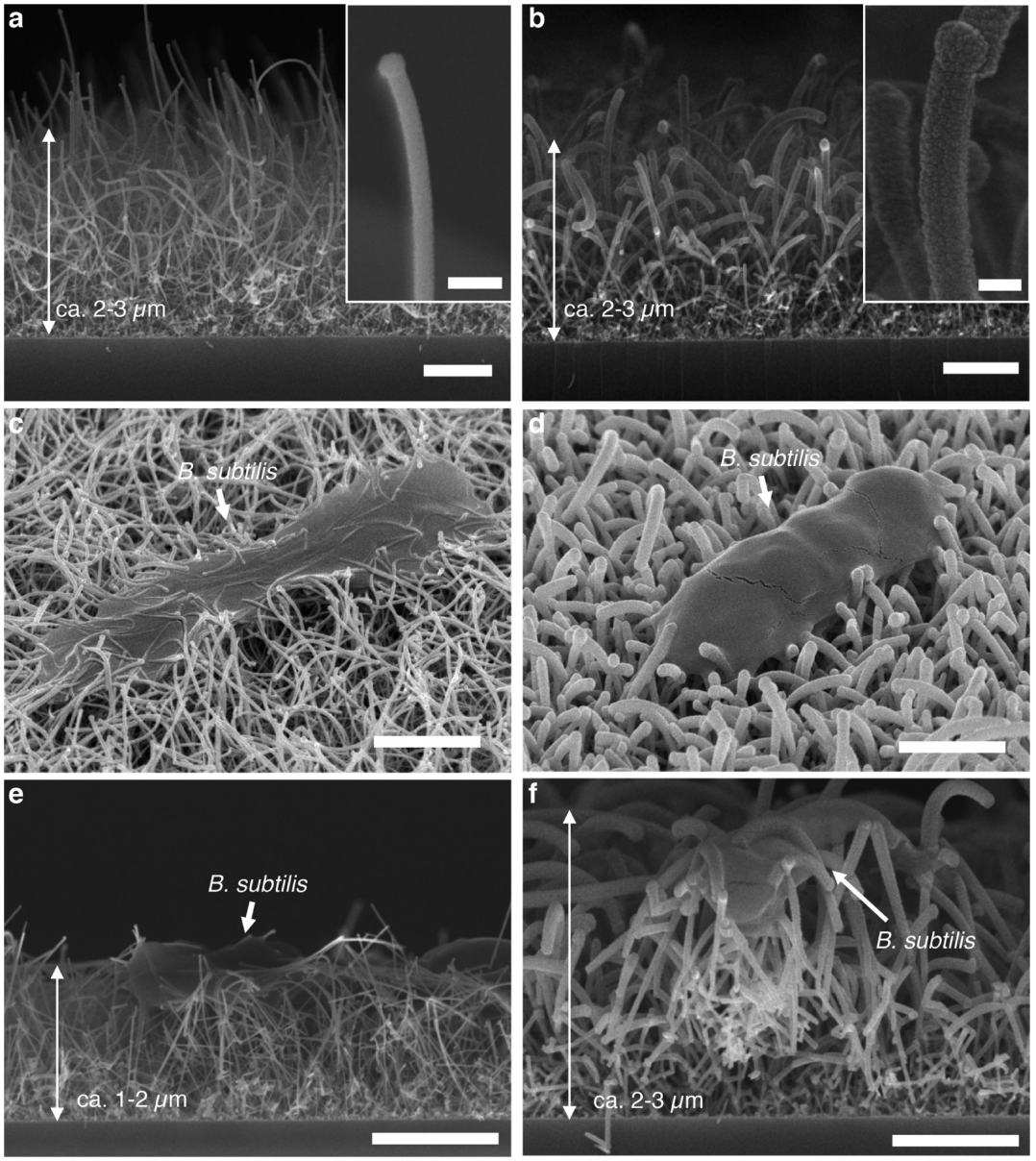

Figure 4. FESEM images of *B. subtilis* deposited onto nanowires (left, 30 nm diameter; right, 110 nm diameter). (a, b) FESEM images showing nanowires of each diameter and 2−3 μm length; scale bars, 1 μm. The inset FESEM images are an enlarged image of each diameter nanowire; scale bars, 100 nm. (c, d) FESEM images that show embedding of *B. subtilis* onto each diameter nanowire; scale bars, 1 μm. (e, f) FESEM images of each diameter nanowire after *B. subtilis* deposition; scale bars, 1 μm.

evaluated whether the substrate had a bactericidal or a bacteria-compatible activity based on colony formation. After exposing each substrate type, we determined the bacteria formed around 100 colonies on SiO_2 substrates and over 250 colonies on SnO_2 substrates, and we calculated their respective bacteria recovery rate as around 30% and 100% (Figure 3a); SnO_2 substrates seemed to have better bacteria-compatible activity than SiO_2 substrates. However, since the antibacterial test has underlying assumptions that give little thought to bacteria adsorption, the substrates with a bacteria adsorption property seem to have false-positive bactericidal activity (a low bacteria recovery rate). In the antibacterial test, some bacteria were not fully removed but rather were attached onto the SiO_2 substrates after washing processes (Figure 3b,c). Considering the well-known bio-compatibility of SiO_2[35] and bacteria adsorption onto SiO_2 substrates, we could conclude that bacteria compatibility for SiO_2 was comparable to or less than that for SnO_2, but the surface coating of SiO_2 could significantly enhance bacteria adsorption. It is noteworthy that the present nanowire materials (core/shell: SnO_2/SiO_2) have bacteria compatibility and enhance microbial cell adsorption onto the nanowires, leading to the efficient initiation of the nanowire-mediated lysis.

The second step for entangling cells with the nanowires was evaluated by the SEM observations showing that the nanowire flexibility (diameter) had an effect on bacteria entanglement (Figure 4, Figures S6−S10). We fabricated SnO_2 nanowires (10 nm in diameter) with a 10 nm or a 50 nm-thick SiO_2 shell layer for flexible or rigid nanowires (Figure 4a,b, Figures S6−S8). These SEM images also showed that the nanowires could have bacteria compatibility. The 30 nm diameter nanowires (core/shell: 10 nm SnO_2/10 nm SiO_2) easily deformed their structure by sticking to the bacteria through their mechanical flexibility

DOI: 10.1021/acsnano.8b08959
ACS Nano 2019, 13, 2262−2273

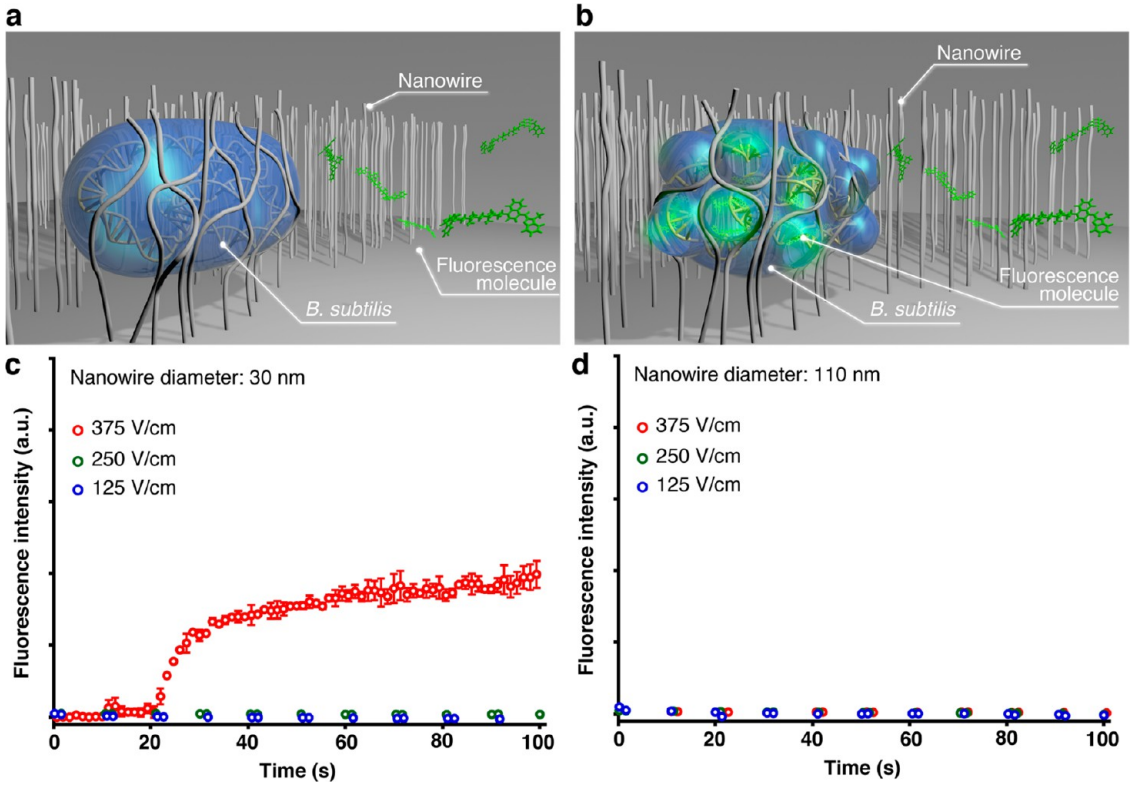

Figure 5. Nanowire-induced microbial cell membrane rupture. (a) A schematic illustration that shows embedding of *B. subtilis* onto the nanowires in a microchannel. (b) A schematic illustration that shows emitted fluorescence intensity of fluorescence molecules by combining them with DNA molecules inside the bacteria after the *B. subtilis* membrane ruptured under application of an electric field. (c) Time-course monitoring of fluorescence intensity inside a single *B. subtilis* using nanowires with a 30 nm diameter. The time 0 s was an interaction point between the cells and nanowires. The microbial cells in the microchannel without nanowires were moved electrophoretically to the anode. Error bars show the standard deviation for a series of measurements (N = 3). (d) Time-course monitoring of fluorescence intensity inside a single *B. subtilis* using nanowires with a 110 nm diameter. Error bars show the standard deviation for a series of measurements (N = 3).

(Figure 4c,e, Figure S9); on the other hand, the 110 nm diameter nanowires (core/shell: 10 nm SnO_2/50 nm SiO_2) did not structurally deform by sticking to the bacteria because of their mechanical stability (Figure 4d,f, Figure S10). Although these SEM images were taken after drying out the samples, it is likely that the mechanical flexibility of the bacteria-compatible nanowires when present in a liquid environment should behave similarly with respect to bacteria entanglement. These results highlight the behavior that the microbial cells introduced by capillary force onto the 30 nm diameter nanowires are absorbed onto the nanowires and then are entangled with the nanowires, leading to progression of the nanowire-mediated lysis.

The third step for stretching the cell membrane was evaluated by monitoring the time series data of fluorescence intensity of labeled DNA molecules showing that the external driving forces (applied electric fields) could rupture the membrane of the entangled bacteria with the 30 nm diameter nanowires or the 100 nm diameter nanowires (Figure 5). It should be noted that we used DNA staining fluorescence molecules, which could not go inside the intact cell membrane (Figure 5a). On the other hand, if the microbial cell can be ruptured solely by the shear force occurring in the spacing between the nanowires under the applied electric field, the fluorescence molecules should go inside the cells from the ruptured membrane and dye nucleic acids inside the cells (Figure 5b). For the applied electric field of 375 V/cm, the 30 nm diameter nanowires could rupture the microbial cell membrane (Figure 5c); on the other hand, under the same applied electric field, the 110 nm diameter nanowires could not rupture it (Figure 5d). The strength of the electric field can control the strength of the pressing force, and then the electric field can control the degree of membrane stretching; the 375 V/cm field is strong enough to make the membrane rupture irreversible, but a field strength <250 V/cm is not. Since the microbial cell membrane in the microchannel with 110 nm diameter nanowires and without them under the applied electric field was not ruptured (it was just moved electrophoretically to the anode), the combination of entangling bacteria with the flexible nanowires and making the shear force in the spacing between the nanowires *via* applying the external driving forces was essential to the completion of the nanowire-mediated lysis of microbial cells.

Nanowire-Mediated Lysis Using Fluid Flow. Since cell adsorption onto the nanowires, cell entanglement with the nanowires, and then cell membrane stretching by the shear force in the spacing between the nanowires are important factors for nanowire-mediated mechanical lysis, we conceived the idea of using fluid flow instead of the applied electric field for extracting and collecting DNA molecules for downstream assays. The nanowire device for fluid flow consisted of nanowires on fused silica substrates and a polydimethylsiloxane (PDMS) microchannel (height, 10 μm) with herringbone structures (height, 3 μm) (Figure 6a,b). The microchannel with herringbone structures can induce chaotic mixing flow,[40] ensuring good convection of solutions. We anticipated that the convection flow could force the microbial cells to contact and entangle with the nanowires and make the shear force in the spacing between

DOI: 10.1021/acsnano.8b08959
ACS Nano 2019, 13, 2262−2273

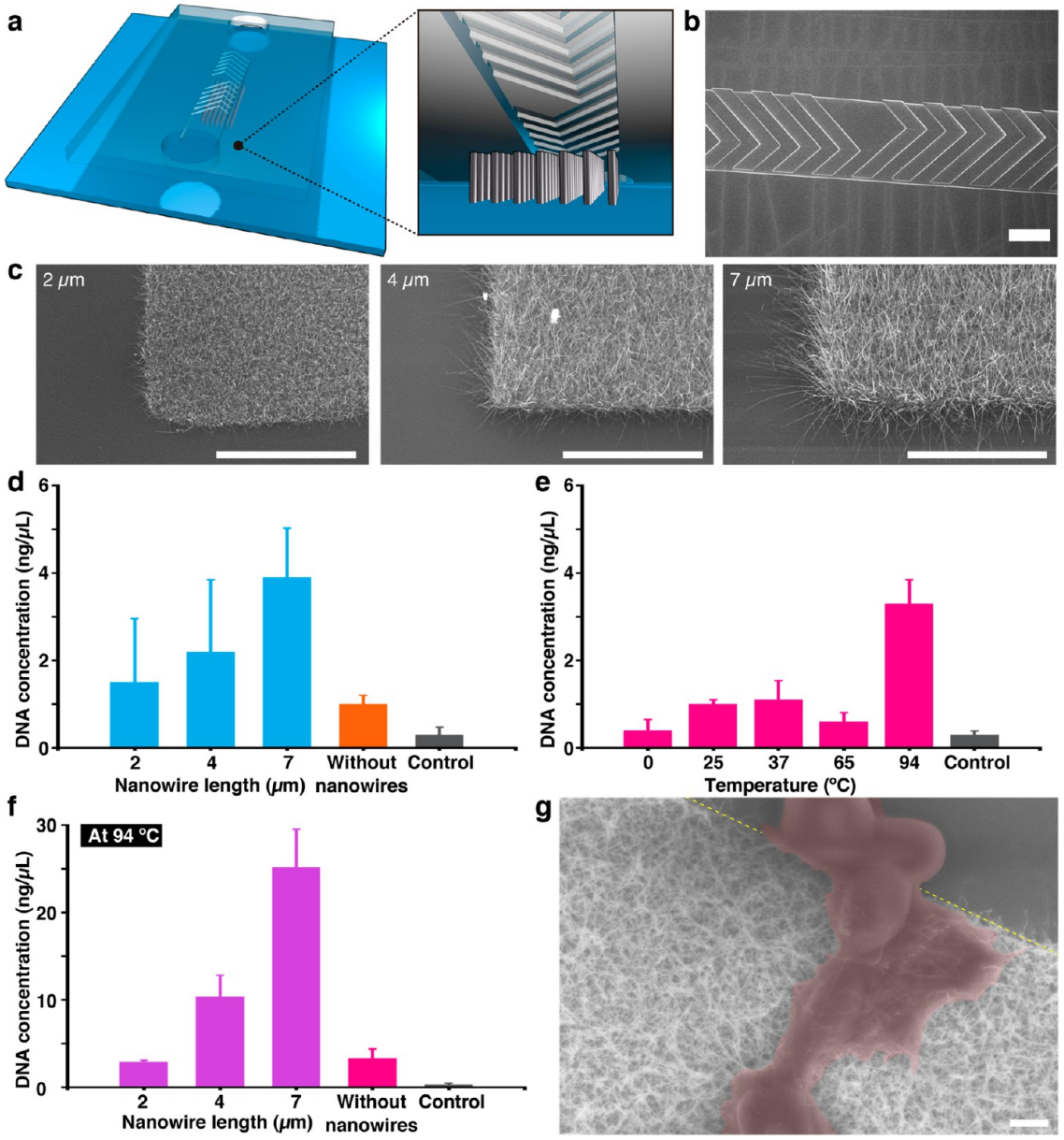

Figure 6. Nanowire-mediated lysis using fluid flow for extracting and collecting DNA molecules. (a) A schematic illustration showing the nanowire device including nanowires and the chaotic mixer. (b) An FESEM image showing the herringbone structures; scale bar, 100 μm. (c) FESEM images showing the nanowire structures (length: 2, 4, and 7 μm); scale bars, 10 μm. (d) Extracted DNA concentration from *S. cerevisiae* cells using the nanowire devices and a microfluidic device with the chaotic mixer (without nanowires). The control had no *S. cerevisiae* cells. Error bars show the standard deviation for a series of measurements ($N = 3$). (e) Extracted DNA concentration from *S. cerevisiae* cells using the microfluidic device with the chaotic mixer (without nanowires) on the Peltier heater at 0, 25, 37, 65, and 94 °C. The control had no *S. cerevisiae* cells. Error bars show the standard deviation for a series of measurements ($N = 3$). (f) Extracted DNA concentration from *S. cerevisiae* cells using the nanowire devices and the microfluidic device with the chaotic mixer (without nanowires) on the Peltier heater at 94 °C. The control had no *S. cerevisiae* cells. Error bars show the standard deviation for a series of measurements ($N = 3$). (g) An FESEM image showing a lysed *S. cerevisiae* cell after nanowire and thermal lysis; scale bar, 1 μm. The lysed cell was highlighted as dark pink, and the boundary between the nanowire and no-nanowire regions was highlighted as the yellow dotted line.

them, leading to membrane stretching and cell rupture (Figure S11). In further anticipation that the nanowire-mediated lysis performance is closely related to the nanowire flexibility, we used the thinner and longer (and therefore, more flexible) nanowires; these were the SnO_2 nanowires without the SiO_2 shell (diameter and length, 10 nm and 2−7 μm, respectively, Figure 6c), since thinner nanowires have higher flexibility,[36,37] and SnO_2 had bacteria compatibility (Figure 3). To demonstrate that the DNA extraction *via* flow-based nanowire-mediated lysis is applicable to much harder microbial cells, we used *Saccharomyces cerevisiae* as a typical example of yeast cells (Supporting Information) which have thick cell walls (200−300 nm)[41,42] against any environmental invasions; the cell walls impose labor-intensive and time-consuming difficulties when treated by yeast cell lysis. Nanowire-mediated lysis using fluid flow allowed us to extract and collect DNA molecules solely by introducing yeast cells, and the extracted amount of DNA molecules had a relationship to nanowire length (Figure 6d). When we used the more densely distributed nanowires (~90−110 wires/μm^2),[9] these were the branched SnO_2 nanowires

DOI: 10.1021/acsnano.8b08959
ACS Nano 2019, 13, 2262−2273

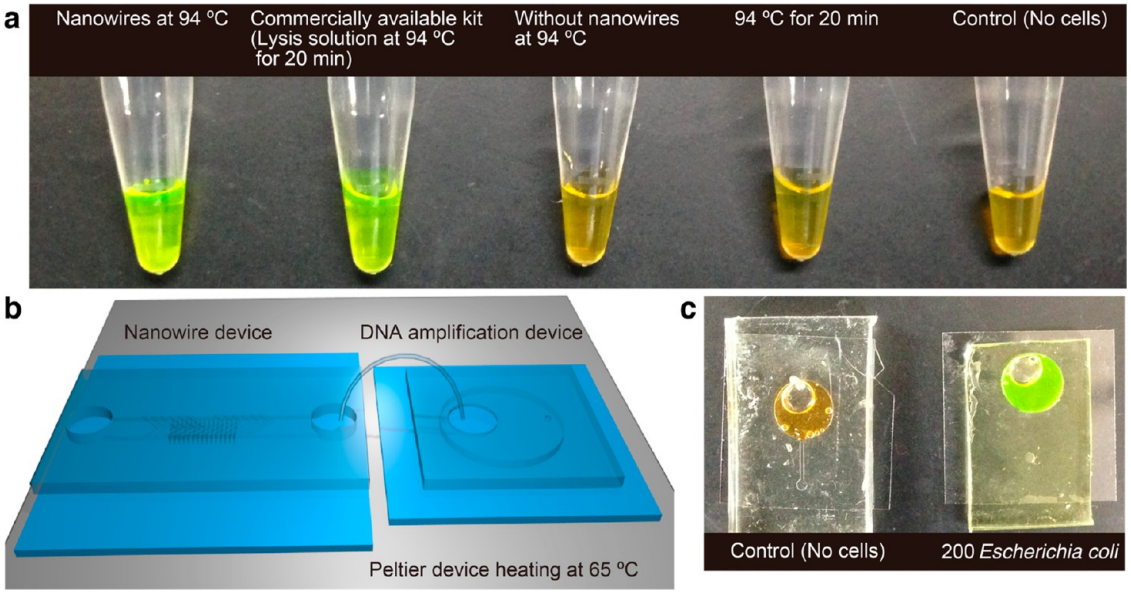

Figure 7. Microbial cell identification using the identification system. (a) A photo of sample tubes after DNA amplification using LAMP in them. While 200 *E. coli* cells exhibited the green fluorescence color when using the nanowire device at 94 °C or a commercially available kit (heated at 94 °C for 20 min after adding lysis solution), 200 *E. coli* cells showed no fluorescence color when using a device without nanowires at 94 °C (only the chaotic mixer) and when heating at 94 °C for 20 min in the sample tubes (without the nanowire device). The control had no *E. coli* cells. (b) A schematic illustration showing the bacteria identification system including the nanowire device and DNA amplification device. Bacteria detection can be realized by introducing a bacteria suspension into the system. (c) A photo of the DNA amplification devices after 60 min. The control had no *E. coli* cells. In the other device, 200 *E. coli* cells exhibited the green fluorescence color.

without the SiO_2 shell (length, 7 and 2 μm for first and second growth, respectively, Figure S12), the extracted amount of DNA molecules was similar to the amount without nanowires. Since the entanglement with the nanowires is a key factor for cell lysis, which is realized by the deformation of the nanowires, it is reasonable that the densely distributed nanowires cannot deform in the confined space and lead to the degradation of cell lysis performance; and therefore, controlling the density distribution of the nanowires is important to achieve a high performance on nanowire-mediated lysis. These results revealed that the nanowire flexibility was closely related to the nanowire-mediated lysis performance. The applicability of flow-based nanowire-mediated lysis to yeast cells could expand diversity of our methodology on the issues of the lysis applicability to all types of microbial cells and the downstream assay applicability to quantitative DNA amplification.

Furthermore, our concept for cell lysis based on oxide nanowire features and fluid flow led us to the idea to incorporate thermal lysis into nanowire-mediated lysis based on the high thermal conductivity of oxide nanowires. As previously reported,[17] thermal lysis under continuous flow conditions has been hindered by the inefficiency of thermal energy transfer from substrate to buffer solution due to low thermal conductivity and the ease of thermal diffusion from the buffer solution to the PDMS microchannel. Since the thermal conductivity of SnO_2 is much higher than that of buffer solution, the nanowires could directly provide thermal energy to yeast cells during the cell adsorption, cell entanglement, or both of them; this concept is completely different from conventional thermal lysis and is another approach that can be facilitated by nanowire-mediated cell lysis. Thermal energy supplied by the nanowires could denature the cell walls and assist the shear force induced by fluid flow, leading to efficient cell ruptures. Compared to only thermal lysis (Figure 6e), the nanowire-mediated thermal and mechanical lysis significantly improved the extraction efficiency of genomic DNA from yeast cells (Figure 6f). After quantifying extracted DNA concentrations (Supporting Information), we obtained their FESEM images by peeling the nanowire device off the PDMS microchannel; these observed results allowed us to confirm the yeast cells were ruptured on the nanowires (Figure 6g). These results have led us to believe that nanowire-mediated lysis will be a powerful tool that offers a strategy to add an additional feature to conventional cell lysis, leading to significantly enhanced lysis performance and overcoming the inherent issues.

Simple, Rapid, and One-Step Identification Assay System. Next, we showed good compatibility of the present nanowire-mediated lysis method with DNA amplification and detection for microbial cell identification. For the identification assay, we used a DNA amplification method based on the loop-mediated isothermal amplification (LAMP),[43] which could amplify our target genes isothermally (Supporting Information). Extracted DNA samples were taken at the nanowire device outlet after introduction of *E. coli*-containing solution into the device, and they showed a chromatic change in the sample tube (Figure 7a). Two hundred *E. coli* cells showed green fluorescence color when using the nanowire device at 94 °C, and this was similar to the result seen in the nanowire-mediated lysis for yeast cells (Figure 6f). On the other hand, 200 *E. coli* cells showed no fluorescence color when using only thermal lysis, such as a chaotic mixer device at 94 °C (no nanowires) and when heating at 94 °C for 20 min in the sample tubes (without the nanowire device); these observations also were similar to those of thermal lysis for yeast cells (Figure 6e). Since 200 *E. coli* cells showed the green fluorescence color when using a commercially available lysis solution at 94 °C for 20 min, nanowire-medicated cell lysis played a similar role to chemical lysis with the lysis objective of 200 *E. coli* cells. These results highlighted that nanowires were important for efficient micro-

DOI: 10.1021/acsnano.8b08959
ACS Nano 2019, 13, 2262−2273

bial cell lysis and the nanowire device had good compatibility with the LAMP method.

Finally, for a simple, rapid and one-step identification assay system, we combined the nanowire device with a DNA amplification device based on the LAMP method (Figure 7b, Supplementary Movie 2). A silicon tube was connected between the outlet of the nanowire device and the inlet of the DNA amplification device. According to the kit manufacturer's instruction manual, DNA polymerase is highly activated at 65 °C when heated for 15−60 min and inactivated at 80 °C when heated for 5 min; therefore, we decided to use a Peltier heater operating at 65 °C. Since the condition of being at 94 °C for 20 min required by the commercially available lysis solution interferes with the DNA polymerase activity, only the nanowire-mediated lysis allows us to premix the LAMP solution with *E. coli*-containing solution before introducing it into the identification system. Thermal lysis at 65 °C showed no significant lysis performance for yeast cells (Figure 6e); therefore, a chromatic change of the LAMP solution should occur when the nanowire-mediated lysis is well-performed on *E. coli* cells. Conversely, a chromatic change of the LAMP solution should not occur when *E. coli* cells are not in solution or the nanowire-mediated lysis does not work well. The identification system showed the green fluorescence color within 60 min (Figure 7c) after introduction of 4 *E. coli* cells/μL in a 50 μL sample volume, in which the LAMP solution was premixed with *E. coli* before introducing it into the identification system. A scenario based on nanowire-mediated mechanical lysis, nanowire-mediated thermal lysis, or both of them can explain the present results. The present concept based on nanowire-mediated lysis has a great potential to achieve simple, rapid, and one-step assay for identification of microbial cells.

CONCLUSION

In summary, we demonstrated a nanowire-mediated lysis method which ruptures cells for Gram-positive and -negative bacteria and yeast cells. Membrane stretching of the microbial cells caused by bacteria-compatible and flexible nanowires plays an important role in attaining nanowire-mediated lysis. In this paper, we demonstrated only nanowire-mediated mechanical and thermal lysis; however, researchers can provide nanowire-mediated chemical, optical, and electrical lysis *via* use of surface-modified nanowires,[44] a nanowire laser[45] or a waveguide,[46] and nanowire electrodes,[47] respectively. These nanowire-mediated lysis methods have a potential to overcome the inherent issues related to chemical, optical, and electrical lysis. Additionally, the nanowire-mediated lysis is readily compatible with various analysis tools because the lysis is triggered by simply introducing the microbial cells. We demonstrated identification of microbial cells based on a chromatic change just by introducing premixed solution into the identification assay system, which could perform DNA extraction, amplification and detection, sequentially. This level of versatility cannot be attained by other methodologies. Since the present method allows users to perform lysis of microbial cells, such nanowire-mediated lysis will offer a strategy to develop analytical systems not only for cell identification but also for on-site detection in a closed system without any contamination.

MATERIALS AND METHODS

Fabrication of Nanowires in a Microchannel. For fabrication of nanowires in a microchannel, we utilized a conventional photolithography process, electron beam lithography, and a vapor−liquid−solid (VLS) growth technique (Figure S1). First, a 250 nm-thick chromium layer was deposited on fused silica substrates using an RF sputtering apparatus (Sanyu Electron Co.) (Figure S1a,b). Positive photoresist TSMR V50 (Tokyo Ohka Kogyo Co.) was spin-coated on the substrates (Figure S1c). Then the microchannel pattern, with a length and width of 8000 and 100 μm, respectively, was formed by photolithography. After development of the resist (Figure S1d), the patterned area was etched by immersing in chromium etchant solution (H_2O:$Ce(NH_4)_2(NO_3)_6$:$HClO_4$, 85:10:5 by weight percent) for 5 min (Figure S1e). The microchannel was etched using a reactive ion etching system (Samco Co.) under CF_4 gas ambient (Figure S1f). The microchannel depth was controlled to 2 μm. After cleaning to remove resist and metal residues (Figure S1g), the inlet and outlet *via* holes (2 mm in diameter) for the microfluidic system were drilled with an ultrasonic driller (Shinoda Co.). We also patterned metal catalysts to define the spatial position of the nanowires within the microchannel. A 10 nm-thick chromium layer was deposited on the substrates (Figure S1h). Electron-beam positive resist ZEP520 A7 (Zeon Corp.) was coated on the microchannel by spin-coating (Figure S1i), and then the pattern was drawn by an electron beam lithography apparatus (Sanyu Electron Co.). After developing the resist (Figure S1j), the chromium layer was patterned by using the chromium etchant solution (Figure S1k). A 3 nm-thick gold layer for nanowire growth was deposited on the substrates using a DC sputtering system (Sanyu Electron Co.) (Figure S1l). Then the chromium layer was removed using chromium etchant solution (Figure S1m). The SnO_2 nanowires were grown from gold catalyst particles that were deposited in a layer formed using a pulse laser deposition (PLD) system (Figure S1n). Details of the nanowire fabrication conditions can be found elsewhere.[48] A 10 nm or a 50 nm-thick SiO_2 shell was deposited onto the SnO_2 nanowires using RF sputtering (Figure S1o). Finally, the microchannel was sealed using a fused silica cover plate (130 μm thick) by the literature method (Figure S1p).[8,10,49]

***Bacillus subtilis* Preparation.** We cultured *B. subtilis* spore (ATCC6633) in 2 mL of 2.5% LB medium (Sigma-Aldrich, Co.) overnight at 37 °C using a multi shaker (Tokyo Rikakikai Co., Ltd.) at a shaking speed of 125 rpm. Then, the *B. subtilis* was applied to LB agar medium (2% agar (Wako Pure Chemical Industries, Ltd.) in 2.5% LB medium), and colonies were allowed to form. After forming the colonies, they were put into 2 mL of fresh 2.5% LB medium and cultured overnight at 37 °C using the multi shaker (shaking speed, 125 rpm). Next, we added 10 μL of the cultured *B. subtilis* to 2 mL of fresh 2.5% LB medium, and we continued the culturing for 5 h at the same temperature and shaking speed. Then, we removed 1 mL of the *B. subtilis* solution and centrifuged it for 10 min at 25 °C and relative centrifugal force (rcf) of 5000*g*. We discarded 1 mL of the supernatant, then added 1 mL of 10 mM phosphate buffer solution, and centrifuged this for 10 min at the same temperature and rcf. After that, we discarded 1 mL of the supernatant again, then added 1 mL of 10 mM phosphate buffer solution, and centrifuged for 10 min for a third time at the same temperature and rcf. Finally, we discarded 1 mL of supernatant and then suspended the *B. subtilis* in 500 μL of 10 mM phosphate buffer solution. We measured optical density (OD) and concentrations of the *B. subtilis* solution by using a POLARstar OPTIMA plate reader (BGM Labtech. Ltd.) at 584 nm and a qNano particle analyzer (Meiwafosis, Co., Ltd.). The *B. subtilis* solution concentrations were diluted as desired in subsequent experiments.

***Escherichia coli* Preparation.** *E. coli* DH5α competent cells (Nippon Gene Co., Ltd.) were applied to LB agar medium (1.5% agar in 2.5% LB medium), and colonies were formed. The formed colonies were put in 2 mL of 2.5% LB medium and cultured overnight at 37 °C with the multi shaker (shaking speed, 125 rpm). Then, we measured the OD of the *E. coli* solution using the plate reader and diluted the *E. coli* using 10 mM phosphate buffer to 0.4 of the measured OD. We centrifuged the diluted *E. coli* solution (10 min; 25 °C; 5000*g*), discarded the supernatant, and suspended the cells in 10 mM phosphate buffer. The concentration (3.9×10^8 *E. coli* cells/mL) in the suspended solution was measured using the qNano particle analyzer.

Observation of *B. subtilis* under a Microscope. We stained the nucleic acid of the *B. subtilis* using 1 μM of SYTO-9 (Life Technologies,

DOI: 10.1021/acsnano.8b08959
ACS Nano 2019, 13, 2262−2273

Ltd.) for 30 min. Then, we centrifuged the *B. subtilis* solution (10 min; 25 °C; 5000*g*). After discarding the supernatant, we added 100 μL of phosphate buffer. Finally, we stained the cell membrane using 5 μg/mL of FM1-43FX (Life Technologies, Ltd.). We observed the *B. subtilis* with a confocal microscope DMI6000B (Leica, Ltd.) (Figure S2a–c). The excitation wavelengths of the microscope laser were 488 and 514 nm for SYTO-9 and FM1–43FX, respectively, and their respective observed emission wavelengths were 495–520 nm and 600–650 nm. We also used the JSM-7610F (Jeol) to capture the field emission scanning electron microscopy (FESEM) images, one example of which is shown in Figure S3d.

DNA Extraction from *B. subtilis* on Nanowires in a Microchannel. We added 500 nM YOYO-1 (Life Technologies, Ltd.) to 3.0×10^8 *B. subtilis* cells/mL in phosphate buffer. Then, we supplied 1 μL of 3.0×10^6 *B. subtilis* cells/mL to the sample reservoir on the nanowire device (Figure S2). After filling the channel with the 3.0×10^6 *B. subtilis* solution, we removed 0.8 μL of the solution and then supplied 2 μL of phosphate buffer containing 500 nM YOYO-1. The high voltage for electrophoresis was controlled from an HVS448 high voltage sequencer (LabSmith) through a platinum electrode which was precisely positioned on the stage of an Eclipse TE-300 inverted microscope (Nikon). A high-pressure mercury lamp was used as an optical source to illuminate DNA molecules at the detection point, and the emitted fluorescence was collected with a C7190–43 EB-CCD camera (Hamamatsu Photonics K.K.) through a 100×/1.40NA objective lens. The excitation wavelength was 450–490 nm, and the emission wavelength was 520 nm. All images were recorded with a DSR-11 digital videocassette recorder (Sony), and then the fluorescence intensity was analyzed by Cosmos32 image-processing software (Library Co., Ltd.).

DNA Extraction from *E. coli* on Nanowires in a Microchannel. We added 500 nM YOYO-1 to 3.0×10^8 *E. coli* cells/mL. Then, we supplied 1 μL of 3.0×10^6 *E. coli* cells/mL to the sample reservoir on the nanowire device. After filling the channel with the 3.0×10^6 *E. coli* solution, we removed 0.8 μL of the solution and then supplied 2 μL of phosphate buffer containing 500 nM YOYO-1. The high voltage for electrophoresis was controlled from the high-voltage sequencer through the platinum electrode which was precisely positioned on the stage of the inverted microscope. The high-pressure mercury lamp was used as the optical source to illuminate DNA molecules at the detection point, and emitted fluorescence was collected with the EB-CCD camera through the 100×/1.40NA objective lens. The excitation laser wavelength range was 450–490 nm, and the observed emission wavelength was 520 nm. All images were recorded with the digital videocassette recorder, and then the fluorescence intensity was analyzed by the Cosmos32 image-processing software.

Antibacterial Test. We carried out a Japanese Industrial Standards (JIS)-based antibacterial test (JIS Z2801, ISO 22916) for SiO_2 and SnO_2 substrates. Each substrate was immersed in ethanol for 10 min before use. Polyethylene film squares (40×40 mm^2) to facilitate bacteria solution spreading onto the substrates were also cleaned in ethanol before their use. A 250 μL aliquot of suspended microbial cells (1.0×10^6 cells/mL) was dropped onto the substrates which had been put into sterile Petri dishes (AGC Techno Glass Co., Ltd.), and then the polyethylene film squares were placed onto the substrates to spread the suspended cells over the entire surface. The Petri dishes with the substrates were transferred into highly humid containers, into which 200 mL sterile water had been added, and the cells were incubated at 35 °C for 24 h. After incubation, the substrates were cleaned using SCDLP culture medium (Eiken Chemical Co., Ltd.). Next, 10 mL of SCDLP culture medium was introduced in between the substrates and the polyethylene films, and then the medium was recovered. After that, the substrates were rinsed by the recovered medium, and then the medium was recovered again. This rinsing process was repeated at least five times. Next, the recovered medium was diluted 100-fold, and then 1 mL of the 100-fold diluted recovered medium (totally, 1000-fold dilution) was mixed with 15 mL of 0.035% Pearlcore nutrient agar, which had been kept at 48 °C, and this medium mixture was put into sterile Petri dishes. After solidifying at room temperature, the dishes were put into an incubator at 35 °C for 48 h. A series of measurements ($N = 3$) were done for SiO_2 and SnO_2 substrates, and 94/84/30 and >250/>250/>250 colonies were observed for SiO_2 and SnO_2 substrates, respectively. The bacteria recovery rate (%) was calculated using the relationship: (observed colonies/250) × 100 (Figure 3a). For confocal microscope images without PBS washing process (Figure 3b), after peeling off the polyethylene film, 250 μL of PBS including SYTO9 (volume ratio: PBS, 1000 μL; SYTO9, 3 μL) was introduced onto the substrates. Finally, another polyethylene film was placed covering the SiO_2 substrates before incubating at 35 °C for 5 min, followed by confocal fluorescence observation. For confocal microscope images with the PBS washing process (Figure 3c), after peeling off the polyethylene film, 10 mL of PBS, instead of SCDLP culture medium, was introduced onto the substrates, and then, 250 μL of PBS including SYTO9 (volume ratio: PBS,1000 μL; SYTO9, 3 μL) was introduced onto the substrates. Finally, another polyethylene film was placed covering the SiO_2 substrates before incubating at 35 °C for 5 min, followed by confocal fluorescence observation.

SEM and STEM Imaging and EDS Mapping. The morphology and the composition of SnO_2/SiO_2 core–shell nanowires were characterized by FESEM, scanning transmission electron microscopy (STEM), and energy dispersive X-ray spectroscopy (EDS). For the cross-sectional SEM-EDS analysis, we utilized an accelerating voltage of 10 kV. For the single-nanowire STEM-EDS analysis, we used an accelerating voltage of 30 kV. The EDS mapping images were 512 × 384 pixels, and the delay time for each pixel was 0.1 ms. The images were integrated for 100 cycles. The peaks of Si Kα (1.739 keV), Sn Lα (3.443 keV), and O Kα (0.525 keV) were chosen to construct the elemental mapping images. The SEM-EDS analysis of *B. subtilis* deposited onto SnO_2/SiO_2 core–shell nanowires was done at an accelerating voltage of 5 kV. We put *B. subtilis* solution onto nanowires on the fused silica substrates and evaporated the solution, and then we observed the SEM images of *B. subtilis*. The SEM images were taken from raw samples, while the 10 nm Pt deposited samples were sometimes used to discriminate the surface morphologies. The EDS mapping images were 512 × 384 pixels, and the delay time for each pixel was 0.1 ms. The images were integrated for 100 cycles. The peaks of Si Kα (1.739 keV), Sn Lα (3.443 keV), O Kα (0.525 keV), and C Kα (0.277 keV) were chosen to construct the elemental mapping images.

Fabrication of Nanowire Device for Fluid Flow. For fabrication of the microchannel with herringbone structures, negative photoresist of SU-8 (3005, Microchem Corp.) was coated on a 3-in. Si wafer (Cretec Kogyo) using a spinner. After baking at 95 °C for 3 min, the microchannel was patterned by photolithography. The microchannel had a length, width, and height of 4000, 200, and 10 μm, respectively. Then, the substrate was baked at 65 °C for 1 min and next at 95 °C for 2 min. The baked substrate was set on the spinner and coated again with 3005 SU-8. The coated substrate was heated at 95 °C for 2 min, and herringbone structures were patterned by photolithography. After baking at 65 °C for 1 min and 95 °C for 1 min, the SU-8 pattern was developed using SU-8 developer (Microchem Corp.) and rinsed with 2-propanol. Polydimethylsiloxane (PDMS) was poured into the SU-8 mold. After degassing, the mold was heated at 80 °C for 2 h. Nanowires were fabricated on fused silica substrates by the VLS method. The nanowire diameter was about 10 nm. The nanowire length was controlled by the VLS growth time. The nanowires on the substrate and the fabricated PDMS microchannel were plasma-treated and bonded to each other at 80 °C.

***Saccharomyces cerevisiae* Preparation.** *S. cerevisiae* (S288C, Open Biosystems) was applied to YPD (yeast extract-peptone-dextrose, MP Biomedicals, Llc.) agar medium (2% agar in 5% YPD medium), and colonies were allowed to form. After forming the colonies, a single colony was put into 5 mL of fresh 5% YPD medium and cultured for 12 h at 30 °C using the multi shaker (shaking speed, 240 rpm). Next, we added 1 mL of the cultured *S. cerevisiae* to 3 mL of fresh 5% YPD medium, and we continued the culturing for 4 h at the same temperature and shaking speed. Then, we measured OD of *S. cerevisiae* solution using the plate reader at 600 nm and diluted the *S. cerevisiae* solution using 5% YPD medium to 0.6 of the measured OD. We centrifuged the diluted *S. cerevisiae* solution (3 min; 25 °C; 15000*g*), discarded the supernatant and suspended the cells in 10 mM phosphate

DOI: 10.1021/acsnano.8b08959
ACS Nano 2019, 13, 2262–2273

buffer. The concentration (1.8×10^7 *S. cerevisiae* cells/mL) in the suspended solution was measured using the cell counter.

Quantifying Extracted DNA Concentrations from *S. cerevisiae* Cells. Extracted DNA concentrations from *S. cerevisiae* cells were calculated from measurements by a spectrophotometer (NanoDrop, Thermo Fisher Scientific Inc.). We centrifuged 200 μL of the *S. cerevisiae* (1.8×10^7 cells/mL) solution (3 min; 25 °C; 15000*g*), discarded the supernatant, and suspended the cells in 200 μL of 2.5 mg/mL Zymolyase (Nacalai Tesque Inc.). Then, we incubated the suspended solution for 10 min at 37 °C, 10 min at 94 °C, 5 min at −80 °C, and 15 min at 94 °C. We centrifuged the solution (3 min; 25 °C; 15000*g*) and recovered the supernatant as extracted DNA solution. We applied quantitative PCR (qPCR) to the recovered solution and depicted a calibration curve for cycle number *vs* extracted DNA concentrations. We quantified extracted DNA concentrations from yeast cells *via* the calibration curve.

Loop-Mediated Isothermal Amplification (LAMP) Method. The LAMP method is an isothermal DNA amplification method, and it uses four kinds of primers and six targeted genes. Mixing samples, primers, DNA polymerase, and substrates were at a constant temperature (around 65 °C) when the LAMP reaction was initiated. Amplification efficiency was high enough to produce 10^9−10^{10} copies for 15−60 min. Specificity was also high enough to distinguish whether the targeted genes were in samples or not. The LAMP method was done using an *E. coli* detection kit (Eiken Chemical Co., Ltd.). According to the kit manufacturer's instruction manual, each *E. coli* detection was performed as follows.

Nanowires at 94 °C (Figure 7a): 50 μL of *E. coli*-containing solution was introduced into the nanowire device at a flow rate of 5 μL/min. The device was put on the Peltier heater and heated at 94 °C. Fifteen μL of the 50 μL *E. coli*-containing solution was collected from the outlet of the device and mixed with 15 μL of LAMP solution in a sample tube. The mixed solution was heated at 65 °C. After 60 min, 1 μL of SYBR Green I was introduced into the sample tube.

Commercially available kit (Figure 7a): 50 μL of *E. coli*-containing solution and 200 μL of lysis solution (Eiken Chemical Co., Ltd.) were mixed in a sample tube. The mixed solution was heated at 94 °C for 20 min. Fifteen μL of the heated solution and 15 μL of LAMP solution were mixed in another sample tube. This second mixed solution was heated at 65 °C. After 60 min, 1 μL of SYBR Green I was introduced into the sample tube.

Without nanowires at 94 °C (Figure 7a): 50 μL of *E. coli*-containing solution was introduced into a device with the chaotic mixer (without nanowires) at a flow rate of 5 μL/min. The device was put on the Peltier heater and heated at 94 °C. Fifteen μL of the 50 μL *E. coli*-containing solution was collected from the outlet of the device and mixed with 15 μL of LAMP solution in a sample tube. The mixed solution was heated at 65 °C. After 60 min, 1 μL of SYBR Green I was introduced into the sample tube.

94 °C for 20 min (Figure 7a): 50 μL of *E. coli*-containing solution was heated at 94 °C for 20 min. Fifteen μL of the heated solution and 15 μL of LAMP solution were mixed in another sample tube. The mixed solution was heated at 65 °C. After 60 min, 1 μL of SYBR Green I was introduced into the sample tube.

Control (no cells) (Figure 7a): 50 μL of solution without *E. coli* was introduced into the nanowire device at a flow rate of 5 μL/min. The device was put on the Peltier heater and heated at 94 °C. Fifteen μL of the 50 μL *E. coli*-containing solution was collected at the outlet of the device and mixed with 15 μL of LAMP solution in a sample tube. The mixed solution was heated at 65 °C. After 60 min, 1 μL of SYBR Green I was introduced into the sample tube.

200 *Escherichia coli* cells (Figure 7c): 30 μL of *E. coli*-containing solution and 30 μL of LAMP solution were mixed outside the bacteria identification system. Then, 50 μL of the 60 μL mixed solution was introduced into the bacteria identification system at a flow rate of 5 μL/min. The system was put on the Peltier heater and heated at 65 °C (Figure 7b). After 60 min, 1 μL of SYBR Green I was introduced into the DNA amplification device.

Control (no cells) (Figure 7c): 30 μL of solution without *E. coli* and 30 μL of LAMP solution were mixed outside the bacteria identification system. Then, 50 μL of the 60 μL mixed solution was introduced into the bacteria identification system at a flow rate of 5 μL/min. The system was put on the Peltier heater and heated at 65 °C (Figure 7b). After 60 min, 1 μL of SYBR Green I was introduced into the DNA amplification device.

The Bacteria Identification Assay System. The mold for the DNA amplification device was fabricated by an RVS-R1 3D printer (Real Vision Systems Inc.). The mold was 3 mm in diameter and 2 mm in height. PDMS was poured into the silanized mold and treated as mentioned in the Fabrication of Nanowire Device for Fluid Flow section. The bacteria identification assay system was fabricated by connecting the nanowire device and the DNA amplification device using a silicon tube (i.d. 0.64 mm, o.d. 1.19 mm, Helix Medical Llc.).

Peltier Heater. The heater for the microfluidic device was composed of a TEC-12708 Peltier element, an HLE power supply, an SP5R7−576 controller, and an SPT-67 thermocouple sensor (all manufactured by Nihontecmo Co. Ltd.). The thermocouple sensor was fixed onto the Peltier element using thermal grease. The controller maintained the temperature at 65 or 94 °C with the accuracy of ±0.3 °C by proportional-integral-derivative control.

ASSOCIATED CONTENT

Supporting Information

The Supporting Information is available free of charge on the ACS Publications website at DOI: 10.1021/acsnano.8b08959.

(1) Schematic of the fabrication procedure for nanowires in a microchannel; (2) schematic illustrations for experimental procedure of nanowire-mediated lysis; (3) *B. subtilis* imaging; (4) the extracted DNA molecules showing electric field response; (5) an FESEM image and EDS elemental mappings of SnO2 film; (6) FESEM images, EDS elemental mappings, and water contact angle of 30 nm diameter nanowires; (7) FESEM images, EDS elemental mappings, and water contact angle of 110 nm diameter nanowires; (8) a TEM image and STEM images of nanowires; (9) FESEM images of *B. subtilis* deposited onto 30 nm diameter nanowires; (10) FESEM images of *B. subtilis* deposited onto 110 nm diameter nanowires; (11) schematic illustrations for DNA extraction using fluid flow and DNA recovery efficiency from the device; (12) nanowire-mediated lysis using the branched nanowires (PDF)

Movie 1: The electrical responsiveness evinced as DNA elongation and contraction with and without an applied electric field, respectively (MOV)

Movie 2: A simple, rapid and one-step bacteria identification assay system (MOV)

AUTHOR INFORMATION

Corresponding Authors

*E-mail: yasui@chembio.nagoya-u.ac.jp.
*E-mail: yanagida@cm.kyushu-u.ac.jp.
*E-mail: kawai@sanken.osaka-u.ac.jp.
*E-mail: babaymtt@apchem.nagoya-u.ac.jp.

ORCID

Takao Yasui: 0000-0003-0333-3559
Takeshi Yanagida: 0000-0003-4837-5701
Kazuki Nagashima: 0000-0003-0180-816X
Noritada Kaji: 0000-0002-9828-873X

Author Contributions

T. Yasui, T. Yanagida, T.S., K.N., N.K., T.K., and Y.B. planned and designed the experiments. T. Yasui, T. Yanagida, K.O., M.T., and S.R., performed DNA extraction *via* nanowire-mediated

DOI: 10.1021/acsnano.8b08959
ACS Nano 2019, 13, 2262−2273

lysis and data analyses. T. Yasui, K.N., T.S., A.Y., R.M., and Z.Z. performed the antibacterial test using fabricated nanowires and data analyses. T. Yasui, T. Yanagida, M.T., and K.N. performed FESEM observations. T. Yasui, T. Yanagida, M.T., S.R., and T.N. performed bacteria identification assay using the nanowire device with a DNA amplification device based on the LAMP method. T. Yasui, T. Yanagida, T.S., K.O., M.T., K.N., S.R., T.N., D.T., A.Y., R.M., Z.Z., N.K., and M.K. fabricated the experimental setups. T. Yasui, T. Yanagida, K.N., and N.K. wrote the paper.

Notes

The authors declare no competing financial interest.

ACKNOWLEDGMENTS

This research was supported by PREST (JPMJPR151B), JST, the JSPS Grant-in-Aid for Young Scientists (A) 17H04803, the ImPACT Program of the Council for Science, Technology, and Innovation (Cabinet Office, Government of Japan), the JSPS Grant-in-Aid for Scientific Research (A) 16H02091, and the Cabinet Office, Government of Japan and the Japan Society for the Promotion of Science (JSPS) through the Funding Program for World-Leading Innovative R&D on Science and Technology (FIRST Program), the Nanotechnology Platform Program (Molecule and Material Synthesis) of the Ministry of Education, Culture, Sports, Science and Technology (MEXT), and the Cooperative Research Program of "Network Joint Research Center for Materials and Devices."

REFERENCES

(1) Rahong, S.; Yasui, T.; Kaji, N.; Baba, Y. Recent Developments in Nanowires for Bio-Applications from Molecular to Cellular Levels. *Lab Chip* **2016**, *16*, 1126−1138.

(2) Qing, Q.; Jiang, Z.; Xu, L.; Gao, R. X.; Mai, L. Q.; Lieber, C. M. Free-Standing Kinked Nanowire Transistor Probes for Targeted Intracellular Recording in Three Dimensions. *Nat. Nanotechnol.* **2013**, *9*, 142−147.

(3) Liu, J.; Fu, T. M.; Cheng, Z. G.; Hong, G. S.; Zhou, T.; Jin, L. H.; Duvvuri, M.; Jiang, Z.; Kruskal, P.; Xie, C.; Suo, Z. G.; Fang, Y.; Lieber, C. M. Syringe-Injectable Electronics. *Nat. Nanotechnol.* **2015**, *10*, 629−637.

(4) Yasui, T.; Yanagida, T.; Ito, S.; Konakade, Y.; Takeshita, D.; Naganawa, T.; Nagashima, K.; Shimada, T.; Kaji, N.; Nakamura, Y.; Thiodorus, I. A.; He, Y.; Rahong, S.; Kanai, M.; Yukawa, H.; Ochiya, T.; Kawai, T.; Baba, Y. Unveiling Massive Numbers of Cancer-Related Urinary-Microrna Candidates *Via* Nanowires. *Sci. Adv.* **2017**, *3*, e1701133.

(5) Rahong, S.; Yasui, T.; Yanagida, T.; Nagashima, K.; Kanai, M.; Klamchuen, A.; Meng, G.; He, Y.; Zhuge, F.; Kaji, N.; Kawai, T.; Baba, Y. Ultrafast and Wide Range Analysis of DNA Molecules Using Rigid Network Structure of Solid Nanowires. *Sci. Rep.* **2015**, *4*, 525.

(6) Xu, A. M.; Aalipour, A.; Leal-Ortiz, S.; Mekhdjian, A. H.; Xie, X.; Dunn, A. R.; Garner, C. C.; Melosh, N. A. Quantification of Nanowire Penetration into Living Cells. *Nat. Commun.* **2014**, *5*, 3613.

(7) Duan, X. J.; Gao, R. X.; Xie, P.; Cohen-Karni, T.; Qing, Q.; Choe, H. S.; Tian, B. Z.; Jiang, X. C.; Lieber, C. M. Intracellular Recordings of Action Potentials by an Extracellular Nanoscale Field-Effect Transistor. *Nat. Nanotechnol.* **2012**, *7*, 174−179.

(8) Yasui, T.; Kaji, N.; Ogawa, R.; Hashioka, S.; Tokeshi, M.; Horiike, Y.; Baba, Y. Arrangement of a Nanostructure Array to Control Equilibrium and Nonequilibrium Transports of Macromolecules. *Nano Lett.* **2015**, *15*, 3445−3451.

(9) Rahong, S.; Yasui, T.; Yanagida, T.; Nagashima, K.; Kanai, M.; Meng, G.; He, Y.; Zhuge, F. W.; Kaji, N.; Kawai, T.; Baba, Y. Three-Dimensional Nanowire Structures for Ultra-Fast Separation of DNA, Protein and Rna Molecules. *Sci. Rep.* **2015**, *5*, 10584.

(10) Yasui, T.; Rahong, S.; Motoyama, K.; Yanagida, T.; Wu, Q.; Kaji, N.; Kanai, M.; Doi, K.; Nagashima, K.; Tokeshi, M.; Taniguchi, M.; Kawano, S.; Kawai, T.; Baba, Y. DNA Manipulation and Separation in Sublithographic-Scale Nanowire Array. *ACS Nano* **2013**, *7*, 3029−3035.

(11) Tuson, H. H.; Auer, G. K.; Renner, L. D.; Hasebe, M.; Tropini, C.; Salick, M.; Crone, W. C.; Gopinathan, A.; Huang, K. C.; Weibel, D. B. Measuring the Stiffness of Bacterial Cells from Growth Rates in Hydrogels of Tunable Elasticity. *Mol. Microbiol.* **2012**, *84*, 874−891.

(12) Stenson, J. D.; Hartley, P.; Wang, C. X.; Thomas, C. R. Determining the Mechanical Properties of Yeast Cell Walls. *Biotechnol. Prog.* **2011**, *27*, 505−512.

(13) Rinke, C.; Schwientek, P.; Sczyrba, A.; Ivanova, N. N.; Anderson, I. J.; Cheng, J. F.; Darling, A.; Malfatti, S.; Swan, B. K.; Gies, E. A.; Dodsworth, J. A.; Hedlund, B. P.; Tsiamis, G.; Sievert, S. M.; Liu, W. T.; Eisen, J. A.; Hallam, S. J.; Kyrpides, N. C.; Stepanauskas, R.; Rubin, E. M.; et al. Insights into the Phylogeny and Coding Potential of Microbial Dark Matter. *Nature* **2013**, *499*, 431−437.

(14) Wilson, M. C.; Mori, T.; Ruckert, C.; Uria, A. R.; Helf, M. J.; Takada, K.; Gernert, C.; Steffens, U. A. E.; Heycke, N.; Schmitt, S.; Rinke, C.; Helfrich, E. J. N.; Brachmann, A. O.; Gurgui, C.; Wakimoto, T.; Kracht, M.; Crusemann, M.; Hentschel, U.; Abe, I.; Matsunaga, S.; et al. An Environmental Bacterial Taxon with a Large and Distinct Metabolic Repertoire. *Nature* **2014**, *506*, 58−62.

(15) Islam, M. S.; Aryasomayajula, A.; Selvaganapathy, P. R. A Review on Macroscale and Microscale Cell Lysis Methods. *Micromachines* **2017**, *8*, 83.

(16) Nan, L.; Jiang, Z. D.; Wei, X. Y. Emerging Microfluidic Devices for Cell Lysis: A Review. *Lab Chip* **2014**, *14*, 1060−1073.

(17) Zhu, K. C.; Jin, H. L.; He, Z. H.; Zhu, Q. H.; Wang, B. A Continuous Method for the Large-Scale Extraction of Plasmid DNA by Modified Boiling Lysis. *Nat. Protoc* **2007**, *1*, 3088−3093.

(18) Schilling, E. A.; Kamholz, A. E.; Yager, P. Cell Lysis and Protein Extraction in a Microfluidic Device with Detection by a Fluorogenic Enzyme Assay. *Anal. Chem.* **2002**, *74*, 1798−1804.

(19) Abolmaaty, A.; El-Shemy, M. G.; Khallaf, M. F.; Levin, R. E. Effect of Lysing Methods and Their Variables on the Yield of Escherichia Coli O157: H7 DNA and Its Pcr Amplification. *J. Microbiol. Methods* **1998**, *34*, 133−141.

(20) Quinto-Su, P. A.; Lai, H. H.; Yoon, H. H.; Sims, C. E.; Allbritton, N. L.; Venugopalan, V. Examination of Laser Microbeam Cell Lysis in a Pdms Microfluidic Channel Using Time-Resolved Imaging. *Lab Chip* **2008**, *8*, 408−414.

(21) Wan, W. J.; Yeow, J. T. W. Study of a Novel Cell Lysis Method with Titanium Dioxide for Lab-on-a-Chip Devices. *Biomed. Microdevices* **2011**, *13*, 527−532.

(22) Jiang, F.; Chen, J. J.; Yu, J. Design and Application of a Microfluidic Cell Lysis Microelectrode Chip. *Instrum. Sci. Technol.* **2016**, *44*, 223−232.

(23) Wang, H.-Y.; Banada, P. P.; Bhunia, A.; Lu, C. Rapid Electrical Lysis of Bacterial Cells in a Microfluidic Device. *Methods in Molecular Biology, Microchip-Based Assay Systems: Methods and Applications*; Floriano, P. N., Ed.; Humana Press: Totowa, NJ, 2007; pp 23−35.

(24) Kido, H.; Micic, M.; Smith, D.; Zoval, J.; Norton, J.; Madou, M. A Novel, Compact Disk-Like Centrifugal Microfluidics System for Cell Lysis and Sample Homogenization. *Colloids Surf., B* **2007**, *58*, 44−51.

(25) Pham, V. T. H.; Truong, V. K.; Mainwaring, D. E.; Guo, Y. C.; Baulin, V. A.; Al Kobaisi, M.; Gervinskas, G.; Juodkazis, S.; Zeng, W. R.; Doran, P. P.; Crawford, R. J.; Ivanova, E. P. Nanotopography as a Trigger for the Microscale, Autogenous and Passive Lysis of Erythrocytes. *J. Mater. Chem. B* **2014**, *2*, 2819−2826.

(26) Di Carlo, D.; Jeong, K. H.; Lee, L. P. Reagentless Mechanical Cell Lysis by Nanoscale Barbs in Microchannels for Sample Preparation. *Lab Chip* **2003**, *3*, 287−291.

(27) Kim, J.; Jang, S. H.; Jia, G. Y.; Zoval, J. V.; Da Silva, N. A.; Madou, M. J. Cell Lysis on a Microfluidic Cd (Compact Disc). *Lab Chip* **2004**, *4*, 516−522.

DOI: 10.1021/acsnano.8b08959
ACS Nano 2019, 13, 2262−2273

(28) Kim, J.; Hong, J. W.; Kim, D. P.; Shin, J. H.; Park, I. Nanowire-Integrated Microfluidic Devices for Facile and Reagent-Free Mechanical Cell Lysis. *Lab Chip* **2012**, *12*, 2914−2921.
(29) So, H. Y.; Lee, K.; Murthy, N.; Pisano, A. P. All-in-One Nanowire-Decorated Multifunctional Membrane for Rapid Cell Lysis and Direct DNA Isolation. *ACS Appl. Mater. Interfaces* **2014**, *6*, 20693−20699.
(30) Ning, R. Z.; Wang, S. Q.; Wu, J.; Wang, F.; Lin, J. M. Zno Nanowire Arrays Exhibit Cytotoxic Distinction to Cancer Cells with Different Surface Charge Density: Cytotoxicity Is Charge-Dependent. *Small* **2014**, *10*, 4113−4117.
(31) Cross, S. E.; Jin, Y. S.; Rao, J.; Gimzewski, J. K. Nanomechanical Analysis of Cells from Cancer Patients. *Nat. Nanotechnol.* **2007**, *2*, 780−783.
(32) Pogodin, S.; Hasan, J.; Baulin, V. A.; Webb, H. K.; Truong, V. K.; Nguyen, T. H. P.; Boshkovikj, V.; Fluke, C. J.; Watson, G. S.; Watson, J. A.; Crawford, R. J.; Ivanova, E. P. Biophysical Model of Bacterial Cell Interactions with Nanopatterned Cicada Wing Surfaces. *Biophys. J.* **2013**, *104*, 835−840.
(33) Ivanova, E. P.; Hasan, J.; Webb, H. K.; Truong, V. K.; Watson, G. S.; Watson, J. A.; Baulin, V. A.; Pogodin, S.; Wang, J. Y.; Tobin, M. J.; Lobbe, C.; Crawford, R. J. Natural Bactericidal Surfaces: Mechanical Rupture of Pseudomonas Aeruginosa Cells by Cicada Wings. *Small* **2012**, *8*, 2489−2494.
(34) Hasan, J.; Webb, H. K.; Truong, V. K.; Pogodin, S.; Baulin, V. A.; Watson, G. S.; Watson, J. A.; Crawford, R. J.; Ivanova, E. P. Selective Bactericidal Activity of Nanopatterned Superhydrophobic Cicada Psaltoda Claripennis Wing Surfaces. *Appl. Microbiol. Biotechnol.* **2013**, *97*, 9257−9262.
(35) Malvindi, M. A.; Brunetti, V.; Vecchio, G.; Galeone, A.; Cingolani, R.; Pompa, P. P. Sio_2 Nanoparticles Biocompatibility and Their Potential for Gene Delivery and Silencing. *Nanoscale* **2012**, *4*, 486−495.
(36) Liang, H. Y.; Upmanyu, M.; Huang, H. C. Size-Dependent Elasticity of Nanowires: Nonlinear Effects. *Phys. Rev. B: Condens. Matter Mater. Phys.* **2005**, *71*, 241403.
(37) Gordon, M. J.; Baron, T.; Dhalluin, F.; Gentile, P.; Ferret, P. Size Effects in Mechanical Deformation and Fracture of Cantilevered Silicon Nanowires. *Nano Lett.* **2009**, *9*, 525−529.
(38) Navarre, W. W.; Schneewind, O. Surface Proteins of Gram-Positive Bacteria and Mechanisms of Their Targeting to the Cell Wall Envelope. *Microbiol. Mol. Biol. Rev.* **1999**, *63*, 174−229.
(39) Costerto, J. W.; Ingram, J. M.; Cheng, K. J. Structure and Function of Cell-Envelope of Gram-Negative Bacteria. *Bacteriol. Rev.* **1974**, *38*, 87−110.
(40) Stroock, A. D.; Dertinger, S. K.; Ajdari, A.; Mezic, I.; Stone, H. A.; Whitesides, G. M. Chaotic Mixer for Microchannels. *Science* **2002**, *295*, 647−651.
(41) Harju, S.; Fedosyuk, H.; Peterson, K. R. Rapid Isolation of Yeast Genomic DNA: Bust N' Grab. *BMC Biotechnol.* **2004**, *4*, 8.
(42) Osumi, M. The Ultrastructure of Yeast: Cell Wall Structure and Formation. *Micron* **1998**, *29*, 207−233.
(43) Notomi, T.; Okayama, H.; Masubuchi, H.; Yonekawa, T.; Watanabe, K.; Amino, N.; Hase, T. Loop-Mediated Isothermal Amplification of DNA. *Nucleic Acids Res.* **2000**, *28*, e63.
(44) Ke, Z. F.; Lin, M.; Chen, J. F.; Choi, J. S.; Zhang, Y.; Fong, A.; Liang, A. J.; Chen, S. F.; Li, Q. Y.; Fang, W. F.; Zhang, P. S.; Garcia, M. A.; Lee, T.; Song, M.; Lin, H. A.; Zhao, H. C.; Luo, S. C.; Hou, S.; Yu, H. H.; Tseng, H. R. Programming Thermoresponsiveness of Nano Velcro Substrates Enables Effective Purification of Circulating Tumor Cells in Lung Cancer Patients. *ACS Nano* **2015**, *9*, 62−70.
(45) Vanmaekelbergh, D.; van Vugt, L. K. Zno Nanowire Lasers. *Nanoscale* **2011**, *3*, 2783−2800.
(46) Yan, R. X.; Park, J. H.; Choi, Y.; Heo, C. J.; Yang, S. M.; Lee, L. P.; Yang, P. D. Nanowire-Based Single-Cell Endoscopy. *Nat. Nanotechnol.* **2012**, *7*, 191−196.
(47) Robinson, J. T.; Jorgolli, M.; Shalek, A. K.; Yoon, M. H.; Gertner, R. S.; Park, H. Vertical Nanowire Electrode Arrays as a Scalable Platform for Intracellular Interfacing to Neuronal Circuits. *Nat. Nanotechnol.* **2012**, *7*, 180−184.
(48) Klamchuen, A.; Yanagida, T.; Nagashima, K.; Seki, S.; Oka, K.; Taniguchi, M.; Kawai, T. Crucial Role of Doping Dynamics on Transport Properties of Sb-Doped SnO_2 Nanowires. *Appl. Phys. Lett.* **2009**, *95*, 053105.
(49) Yasui, T.; Kaji, N.; Mohamadi, M. R.; Okamoto, Y.; Tokeshi, M.; Horiike, Y.; Baba, Y. Electroosmotic Flow in Microchannels with Nanostructures. *ACS Nano* **2011**, *5*, 7775−7780.

DOI: 10.1021/acsnano.8b08959
ACS Nano 2019, 13, 2262−2273